INL/CON-05-00183
PREPRINT

Measurement of Sorption-Induced Strain

2005 International Coalbed Methane Symposium

Eric P. Robertson
Richard L. Christiansen

May 2005

The INL is a
U.S. Department of Energy
National Laboratory
operated by
Battelle Energy Alliance

Measurement of Sorption-Induced Strain

Eric P. Robertson, Idaho National Laboratory
and
Richard L. Christiansen, Colorado School of Mines

ABSTRACT

Strain caused by the adsorption of gases was measured in samples of subbituminous coal from the Powder River basin of Wyoming, U.S.A. and high-volatile bituminous coal from east-central Utah, U.S.A. using an apparatus developed jointly at the Idaho National Laboratory (Idaho Falls, Idaho, U.S.A.) and Colorado School of Mines (Golden, Colorado, U.S.A.). The apparatus can be used to measure strain on multiple small coal samples based on the optical detection of the longitudinal strain instead of the more common usage of strain gauges, which require larger samples and longer equilibration times. With this apparatus, we showed that the swelling and shrinkage processes were reversible and that accurate strain data could be obtained in a shortened amount of time. A suite of strain curves was generated for these coals using gases that included carbon dioxide, nitrogen, methane, helium, and various mixtures of these gases. A Langmuir-type equation was applied to satisfactorily model the strain data obtained for pure gases. The sorption-induced strain measured in the subbituminous coal was larger than the high-volatile bituminous coal for all gases tested over the range of pressures used in the experimentation, with the CO_2-induced strain for the subbituminous coal over twice as great at the bituminous coal.

INTRODUCTION

Coal seams have the capacity to adsorb large amounts of gases because of their typically large internal surface area. Some gases, such as carbon dioxide, have a higher affinity for the coal surfaces than others such as nitrogen. Two gases are of particular importance: methane, because of its inherent value as a fuel; and carbon dioxide, because of its purported effect on global warming.

Fluid Movement in Coal

As reservoir pressure is lowered, gas molecules are desorbed from the matrix and travel to the cleat (natural fracture) system where they are conveyed to producing wells. Fluid movement in coal is controlled by diffusion in the coal matrix and described by Darcy flow in the fracture (cleat) system. Because diffusion of gases through the matrix is a much slower process than Darcy flow through the fracture (cleat) system, coal seams are treated as fractured reservoirs with respect to fluid flow.

Sorption-Induced Strain and Relationship to Permeability

Coalbeds, however, are more complex than other fractured reservoirs because of their ability to adsorb (or desorb) large amounts of gas. Adsorption of gases by the internal surfaces of coal causes the coal matrix to swell and desorption of gases causes the coal matrix to shrink. The swelling or shrinkage of coal as gas is adsorbed or desorbed is referred to as sorption-induced strain. Sorption-induced strain of the coal matrix causes a change in the width of the cleats or fractures that must be accounted for when modeling permeability changes in the system. A number of permeability-change models for coal have

been proposed that include the effect of sorption-induced strain [1,2,3,4,5,6]. Accurate measurement of coal strains induced by the sorption of gases becomes important when modeling the effect of gas sorption on coal permeability.

Previous Strain Measurements with Reported Difficulties

Until recently, sorption-induced strain data that can be incorporated into permeability models have been difficult and tedious to collect; however, recent advancements have allowed for the collection of strain data in a much more timely fashion. The measurement of sorption-induced strain in coal has been reported by a relative few researchers. Gray [1] reported that strain varied linearly with gas pressure for both CO_2 and CH_4, but did not include any details about how those values were obtained. Harpalani and Schraufnagel [7] showed that sorption-induced coal strain was not necessarily a linear function of gas pressure, but might be non-linear with decreasing gas pressure. For a coal sample 1.5 inches in diameter and 3 inches in length and measuring strain with strain gauges they found that the sorption process can be extremely slow requiring long stabilization times.

Seidle and Huitt [3] also used strain gauges to measure the volumetric strain of coal samples subjected to various gases under pressure and noted that the resulting strain tests yielded curves resembling sorption isotherm curves and opined that sorption-induced strain was correlated with sorbed gas content. They found that with the large samples required for measurements using strain gauges, the sorption process was slow, requiring nearly three months to stabilize.

Levine [8] presented both longitudinal and volumetric strain for high-volatile bituminous Illinois coal using both carbon dioxide and methane showing that volumetric strain is roughly three times the longitudinal strain (see also Appendix A for derivation relating longitudinal and volumetric strain). Resistance-type strain gauges also presented some problems that Levine noted: 1) they may not adhere properly to the coal, 2) they may not deform homogeneously with the coal, and 3) the length of time required for equilibration caused by restrictions of the coal sample size could be very long. He noted that some samples required exposure times as long as 200 hours (over 8 days), with larger samples requiring even longer equilibration times; and any measurement errors due to the lack of equilibration would result in measurements lower than reality.

Zutshi and Harpalani [9] presented coal volumetric strain data collected using strain gauges attached to coal samples of unspecified dimensions. The coal samples were placed in vessels and pressurized with various gases. Equilibration times for these tests were long; resulting in total time of about 220 days to collect five data points. Chikatamarla and Bustin [10] also recently reported strain measurements using strain gauges and although they do not mention the amount of time needed for equilibration, they did report problems with gas reacting with the strain gauges forcing an early termination of some experiments.

Table 1 summarizes some coal strain data collected using resistance-type strain gauges as reported by previous researchers.

Need for More Coal Strain Data

In light of the rapid development of coalbed methane plays and the potential for CO_2 storage in unmineable coal seams, very little sorption-induced strain data have been reported. Perhaps this is because of the difficulties associated with resistance-type strain gauges and the length of time required for equilibration of the samples. Clearly, if strain data are to be incorporated into the permeability equations that are employed in coalbed simulators, more sorption-induced strain data are needed. In order to avoid the difficulties encountered by previous researchers and to speed up the data collection process, we wanted to determine if strain could be accurately measured on smaller coal samples without the use of resistance-type strain gauges. The use of smaller samples would conceivably result in shorter equilibration times and faster data collection.

STRAIN MEASUREMENT APPARATUS

An earlier paper by Robertson and Christiansen [11] discusses the development of the strain measurement apparatus used in this research and more detail can be found there regarding the different

ideas tried and how the current version of the apparatus was developed. The apparatus used for measuring coal strain currently includes an optical microscope mounted to a pressure vessel with transparent view ports through which changes in coal length can be optically detected. A brief description of its components and operation follows.

Figure 1 is a photograph of the apparatus developed to measure the longitudinal strain of multiple samples under identical conditions of pressure, temperature, and gas composition. In the photograph, a microscope can be seen attached to the pressure vessel and it is through this microscope that the change in the length of the samples is monitored. The microscope that can be positioned anywhere along the outside of the vessel by turning the positioning screw handle. Two opposite sides of the pressure vessel are composed of thick, yet transparent glass through which the coal samples inside the pressure vessel can be seen with the aid of a backlight. The microscope currently being used has a magnification of 2.3X, which gives an object field of 4.8 mm. The coal samples used in these experiments are roughly 20 mm in length, 3 mm in width, and 3 mm in height (¾ in. by ⅛ in. by ⅛ in.). Because of the magnification of the microscope, only the ends of the samples can be seen. The apparatus is tilted about 45 degrees with respect to the horizontal plane so that the coal samples are at rest at one end of the bed. Monitoring changes in length of the samples' free ends allows the calculation of longitudinal strain. The strain is calculated by comparing the initial end position of each of the samples relative to a static mark with subsequent end positions relative to the same mark at different conditions.

The apparatus is capable of holding six samples that lie in individual beds machined into a stainless steel support rod. The ends of the rod are drilled through to allow gas to enter and exit the pressure vessel when desired. When the samples need to be changed, the entire rod is simply removed from the vessel and new samples are placed in the sample beds and reinserted into the chamber. The lower limit of accurate and repeatable measurements of changes in length is 0.001 mm, which translates into a strain of 0.005% for a 20 mm sample. The upper limit is 4 mm, yielding a strain of 20% for a 20 mm sample, which is an order of magnitude larger than typical coal strain induced by gas adsorption.

Volumetric Strain versus Longitudinal Strain

Volumetric strain is three times the measured longitudinal strain under isotropic conditions (see Appendix A for derivation of this relationship). The assumption of isotropic conditions is supported by the strain results reported by Levine [8]. In his experiments, he recorded strain in the direction of all three dimensions and plotted both longitudinal strain and calculated volumetric strain. The ratio of the longitudinal strain to the volumetric strain in Levine's data is 1:3, which supports the assumption that small samples of coal can be considered isotropic.

COAL DESCRIPTION

The small coal samples used for strain measurement were taken from larger blocks of coal that were collected from coal mines in Utah and Wyoming. The high-volatile bituminous Utah coal was collected from the Aberdeen seam, the Gilson seam, and the lower Sunnyside seam of the Book Cliffs coal field from underground mines near Price, Utah. Subbituminous, low-contaminant coal from the Powder River basin was collected from the Anderson seam and the Canyon seam from an open pit coal mine near Gillette, Wyoming. At the mine location, the Canyon and Anderson seams are each over 100 ft thick and separated by about 150 feet of non productive rock. Proximate, ultimate, and heating value analyses were subsequently done on samples of the collected coal and are shown in Table 2. Literature values obtained for the both the Wyoming coal [12] and the Utah coal [13] are also shown in Table 2 for comparison. Additional coal information can be found in an Argonne National Laboratory study [14] using a Utah coal collected from a mine adjacent to the coal used in this study.

COAL COLLECTION AND SAMPLE PREPARATION

The Utah coal was taken from the conveyer belt carrying recently mined coal out of the mine as close to the active mine face as possible to limit oxygen exposure. Immediately after being taken from the conveyer, each sample was double wrapped in plastic bags and sealed by tape. Transporting the sample from the mine face to the surface took from 5 to 20 minutes depending on the collection site. Upon reaching the surface, the samples were removed from the bags and placed under de-ionized water inside

containers for transport back to the Idaho National Laboratory (INL) in Idaho Falls, Idaho. One coal sample was taken from the Aberdeen mine (Aberdeen seam), one from the Centennial mine (Gilson seam), and two from the West Ridge mine (Sunnyside seam).

The Wyoming coal was collected from recently exposed walls from an open pit mine. Large boulders were broken to expose fresh coal inside and smaller samples (roughly one cubic foot) were then taken from this fresh area and immediately placed under water in sealed containers for transport to the INL. Large coal blocks were taken from the Anderson seam and also from the Canyon seam in this manner.

The large coal blocks were kept underwater at the INL laboratories until needed. The small samples used to measure strain were taken from the larger blocks by using a rock saw cooled by de-ionized water. The small samples were then dried on the lab bench using paper towels, measured, and placed into the strain measurement apparatus. We did not attempt to retain the moisture within the coal samples. The moisture within the samples was evaporated at 80° F inside the strain measurement apparatus by cycling between a vacuum and high pressure moisture- and oxygen-free gas until strain at the pressure extremes was constant.

EXPERIMENTAL PROCEDURE

All strain measurements were done at a constant temperature of 80° F. Initially, a hard vacuum was applied to the pressure chamber for 24 hours and then the initial location of each of the sample ends with respect to specific marks on the measurement standard was recorded. Gas was then introduced into the chamber and pressurized to a desired pressure and changes in the length of the samples were monitored over time as gas was adsorbed by the coal and the samples equilibrated to the new pressure state. The strain of five coal samples were averaged to arrive at an average strain value and one stainless steel sample was used as a control. This procedure was repeated for a number of increasingly higher pressures until the maximum desired pressure was achieved. At that point, a hard vacuum was applied to determine the reversibility of the strain as gas was desorbed. The process was repeated for other gases of interest.

RESULTS AND DISCUSSION

Figure 2 shows the average strain with respect to adsorption time of five Anderson coal samples under differing carbon dioxide pressures. We found that the increase in strain over time at a given pressure could be modeled very well using a Langmuir-type equation. This approach was helpful in determining what the strain would be at infinite time if the strain were not completely stabilized after 24 hours.

Figure 3 shows the same strain data as in Figure 2, but modeled using a Langmuir-type equation of the following form:

$$S = S_t \frac{t}{t_L + t}, \quad \text{Eq (1)}$$

where S is the measured strain, S_t is the equilibrated strain (extrapolated to time = ∞), t is time in hours, and t_L is a constant representing the time at which S equals ½ S_t. Both S_t and t_L are variables determined by the shape of the strain-time data.

The constant t_L can be used as a measure of equilibration time; a small value for t_L means that the strain stabilized rapidly, while a large value for tL represents a long stabilization time. As can be seen in Figure 3, the CO_2 strain data stabilized very quickly at lower pressures (t_L = 0.032 hrs for 100 psia) and the equilibration rate became progressively longer at the higher pressures (t_L = 10.7 hrs at 800 psia). Similar plots showing the relationship between equilibration time and strain stabilization could be constructed for each gas and coal combination, but are not included in this paper due to space constraints.

The strain measurement procedure called for collecting data for 24 hours at each pressure point and then modeling the data using Eq (1) to extrapolate to infinite time. In retrospect, more time could have been allowed at the higher pressure regions of the tests. However, because the data is modeled very well by the Langmuir-type equation, any error associated with the extrapolation is expected to be small. Further testing should be done to determine the reason for the longer equilibration times in the higher pressure region.

The calculated value of S_t at the various pressures was then used to construct a strain versus pressure plot, which can be seen in Figure 4. In this figure the average longitudinal strain of the Anderson seam coal is plotted against pressure under an atmosphere of CO_2.

A Measure of the Associated Error

Figure 4 also shows the measured strain of a non-reactive stainless steel sample of the same size as the coal samples used as a control. Because the control is non-reactive, any measured strain in the control is equivalent to the error associated with the measured strain in the reactive coal samples. The standard deviation of the error (measured strain of control sample) is 0.0016%. The error associated with these measurements appears to be random error resulting from the ability to accurately and repeatedly determine the location of the ends of the samples.

Modeling Strain Data

The strain data in Figure 4 are modeled using a Langmuir-type equation of the following form:

$$S = S_{max} \frac{P}{P_L + P}, \quad \text{Eq (2)}$$

where S is the measured strain, S_{max} is the maximum strain at infinite pressure, P is the gas pressure in psia inside the pressure chamber, and P_L is a constant representing the pressure at which S equals ½ S_{max}. Eq (2) is the same basic equation as Eq (1), but with different constants representing pressure instead of time.

Strain was measured using both the Gilson coal and the Anderson coal as a function of gas pressure for three pure gases: CO_2, CH_4, and N_2. Figure 5 shows the data resulting from these experiments along with the modeling of the data using Eq (2). Table 3 shows the Langmuir strain constants accompanying the model curves for the different coals and gases. The values of P_L are fairly constant for a given gas regardless of the coal rank as seen in Table 3. However, different sorbing gases result in different total strains (S_{max}). Data show that as the total strain decreases, the Langmuir pressure, P_L, increases; meaning that gases with large sorption-induced strains such as CO_2 approach their maximum strain at lower pressures than those with low sorption-induced strains such as N_2.

The relationship between S_{max} and P_L can be seen in Figure 6, which plots the average value of P_L, as a function of the average S_{max} for both the Anderson and Gilson coals. The trend for a declining P_L with an increasing S_{max} is almost linear. The “flattening out” of the strain curve as total strain decreases is analogous to the increase in Langmuir pressure as adsorption decreases as observed by other researchers [10,16].

This figure (Figure 6) also shows data suggesting that the product of Langmuir strain constant and the Langmuir pressure ($S_{max} \cdot P_L$) decreases as S_{max} decreases; and ranges from 14 psia for CO_2 down to 2.8 psia for N_2.

Shape of Sorption-Induced Strain Data

Seidle and Huitt reported pre-1990 coal strain data from several authors suggesting that sorption-induced coal strain varied linearly with pressure [3]. Some early results from Harpalani and Schraufnagel [7] appear to indicate that sorption-induced strain in coal could be linear with respect to pressure. However, our data (Figure 5) clearly indicate that sorption-induced strain is not a linear function of gas pressure, but can be very satisfactorily fit using a Langmuir-type equation. This should be expected because the principal cause of the change in coal dimensions (strain) is the sorption of gas, which is modeled by the Langmuir isotherm.

A secondary cause of strain in these experiments is the gas pressure acting to compress the coal samples. As gas pressure changes, the resulting compressive and sorptive strains are counter acting. The matrix compressive strain is small relative to the sorption-induced strain in the presence of carbon dioxide, but may become important when the sorbed gas is only slightly adsorptive such as nitrogen. The

matrix compressibility can be determined by measuring the strain of a coal sample subjected to the pressure of a non-adsorbing gas such as helium. Figure 7 shows the strain induced by the exposure of the coal samples to helium at various pressures with temperature held constant at 80° F. These data were obtained after allowing sufficient equilibration time to arrive at constant values with respect to time. From the data shown in Figure 6, the longitudinal matrix compressive strain is calculated to be 0.84E-6 psi^{-1}, which translates into a volumetric matrix compressibility of 2.5E-6 psi^{-1} for Anderson (subbituminous) coal at 80° F.

Both adsorption isotherms and strain isotherms can be modeled using forms of the Langmuir equation and it may be possible to predict one based on the character of the other. There is evidence that for most gases and coals, the relationship between strain and adsorption is linear [8,10]. However, Pekot and Reeves suggest that for high adsorbed gas concentration, the adsorption-strain relationship may become non-linear [15]. More work needs to be done in this area before any strong conclusions can be made as to the relationship between strain and adsorption curves, but there is strong evidence that there is a positive (and possibly linear) relationship between the sorption and strain isotherms.

Strain and Coal Rank

The data presented in Figure 5 show a marked difference in the sorption strain between the two ranks of coals studied here. The relationships between sorption-induced strain and coal rank for the three gases used in this study are shown in Figure 8. In this figure, S_{max} (strain at infinite gas pressure) is used as a measure of strain and vitrinite reflectance is used as a measure of coal rank. The CH_4 strain decreases only slightly with the change in coal rank, but the CO_2 and N_2 strain curves each decrease by a factor of about two as vitrinite reflectance increases from 0.24 to 0.53. One would expect the strain curves of all three gases to be affected in the same manner by the change in coals, and more work should be done to determine if the CH_4 data are truly unaffected by a change in coal rank or if it is simply an experimental anomaly.

Regardless of the amount of decrease in strain resulting from an increase in coal rank, the strain of all three gases did decline as rank increased. Other researchers, however, have shown different results. Bustin [16] compared the adsorption capacity of coals of different ranks and found a trend towards higher capacity with higher coal rank. Later, Chikatamarla and Bustin [10] measured sorption-induced strains of various coals and found that strain also increased with higher coal rank, which is contrary to the data reported here (see Figure 8). Based on these results, it may not be possible to derive a general relationship between coal strains (and by analogy, adsorbed gas) and coal rank without further testing on a much larger group of coals of various ranks.

Strain Ratios and Coal Rank

The ratio of strain induced by CO_2 adsorption to strain induced by CH_4 adsorption is of some importance when considering using coal seams as CO_2 sinks for sequestration of carbon or considering CO_2-enhanced CBM production (CO_2-ECBM). During either of these two processes, the strain in the coal increases as CO_2 displaces methane. If the increase in strain is large enough, this can cause a significant reduction in permeability. Figure 9 shows the ratio of CO_2 strain and CH_4 strain for the two coals tested to date. This figure shows that if all the methane in the coal were to be displaced by carbon dioxide, the expected increase in strain would be about twice as large in the subbituminous coal compared to the bituminous coal. Therefore, permeability reduction due to coal swelling during CO_2-ECBM or CO_2 sequestration in coal appears to be sensitive to the rank of the coal and may be more of a detriment in coals of lower rank. This knowledge should be considered during the field selection process for CO_2-ECBM or CO_2 sequestration planning stages.

Reeves [17] compiled some historical data showing a relationship between the CO_2/CH_4 adsorption ratio and coal rank and found that as coal rank increased from subbituminous to high volatile bituminous the CO_2/CH_4 adsorption ratio decreased. However, Chikatamarla and Bustin [10] published strain data showing very little trend in CO_2/CH_4 strain ratio with respect to coal rank. The data shown in Figure 9 tend to support the results presented by Reeves, but definite conclusions regarding the relationship between CO_2/CH_4 strain ratios and coal rank are difficult to make because data for only two coals have been collected to date, and further testing should be done.

CONCLUSIONS

A novel method to measure the longitudinal strain in coal induced by the sorption of gases has been developed that greatly reduces the amount of time required for sample equilibration. The total time needed to obtain data necessary to construct a strain-pressure plot for a given temperature has been reduced from over 100 days with traditional strain gauges to less than 10 days using this new technique.

As sorption pressure increased the equilibration time also increased for the samples tested. Further experimentation should be done to determine the cause for this behavior.

Sorption-induced strain data with respect to time (at constant pressure and temperature) can be modeled using a Langmuir-type equation, which allows the extrapolation of strain data to infinite time. Strain data with respect to adsorption pressure can also be modeled using a Langmuir-type equation and is not a linear function of pressure.

When comparing the strain curves for different gases, CO_2 adsorption caused the highest strain, followed by CH_4, and N_2 adsorption caused the lowest strain in both coals tested. As total strain decreased, the Langmuir pressure, P_L, increased. Gases with large sorption-induced strains such as CO_2 approach their maximum strain at lower pressures than those with low sorption-induced strains such as N_2.

Sorption-induced strain decreased as coal rank increased for all gases tested. The CO_2 and N_2 strains were about twice as large in the subbituminous coal as the high-volatile bituminous coal, while CH_4 strain was only 1.1 times larger in the subbituminous coal than the high-volatile bituminous coal. The CO_2/CH_4 strain ratio also decreased with an increase in coal rank.

Because sorption-induced strain is important to modeling reservoir performance during coalbed CO_2 sequestration, CO_2-ECBM, as well as CBM production by pressure depletion, more strain measurements are needed for a wide variety of coals and under different conditions.

APPENDIX A – DERIVATION OF RELATIONSHIP BETWEEN LONGITUDINAL AND VOLUMETRIC STRAIN

By definition, longitudinal strain,

$$S_L = \frac{\Delta L}{L}, \quad \text{..... Eq (3)}$$

where ΔL is the change in length of a dimension and L is the original length of that dimension. Also by definition, volumetric strain,

$$S_V = \frac{\Delta V}{V}, \quad \text{..... Eq (4)}$$

where ΔV is the change in volume of a body and V is the original volume of that body.

Assume we are given a solid, rectangular box with dimensions L_1, L_2, and L_3. By applying a strain-inducing force in all directions, the change in volume can be calculated by:

$$\Delta V = (L_1 + \Delta L_1)(L_2 + \Delta L_2)(L_3 + \Delta L_3) - L_1 L_2 L_3. \quad \text{..... Eq (5)}$$

Multiplying these terms and simplifying,

$$\Delta V = L_1 L_2 L_3 + L_2 L_3 \Delta L_1 + L_1 L_3 \Delta L_2 + L_1 L_2 \Delta L_3 + L_1 \Delta L_2 \Delta L_3 + L_2 \Delta L_1 \Delta L_3 + L_3 \Delta L_1 \Delta L_2 + \Delta L_1 \Delta L_2 \Delta L_3 - L_1 L_2 L_3; \quad \text{..... Eq (6)}$$

and

$$\Delta V = L_2 L_3 \Delta L_1 + L_1 L_3 \Delta L_2 + L_1 L_2 \Delta L_3 + L_1 \Delta L_2 \Delta L_3 + L_2 \Delta L_1 \Delta L_3 + L_3 \Delta L_1 \Delta L_2 + \Delta L_1 \Delta L_2 \Delta L_3. \quad \text{..... Eq (7)}$$

Volumetric strain then becomes:

$$S_V = \frac{\Delta V}{V} = \frac{L_2 L_3 \Delta L_1 + L_1 L_3 \Delta L_2 + L_1 L_2 \Delta L_3 + L_1 \Delta L_2 \Delta L_3 + L_2 \Delta L_1 \Delta L_3 + L_3 \Delta L_1 \Delta L_2 + \Delta L_1 \Delta L_2 \Delta L_3}{L_1 L_2 L_3}. \quad \text{..... Eq (8)}$$

Simplifying,

$$S_V = \frac{\Delta V}{V} = \frac{L_2 L_3 \Delta L_1}{L_1 L_2 L_3} + \frac{L_1 L_3 \Delta L_2}{L_1 L_2 L_3} + \frac{L_1 L_2 \Delta L_3}{L_1 L_2 L_3} + \frac{L_1 \Delta L_2 \Delta L_3}{L_1 L_2 L_3} + \frac{L_2 \Delta L_1 \Delta L_3}{L_1 L_2 L_3} + \frac{L_3 \Delta L_1 \Delta L_2}{L_1 L_2 L_3} + \frac{\Delta L_1 \Delta L_2 \Delta L_3}{L_1 L_2 L_3}. \quad \text{Eq (9)}$$

Canceling terms,

$$S_V = \frac{\Delta V}{V} = \frac{\Delta L_1}{L_1} + \frac{\Delta L_2}{L_2} + \frac{\Delta L_3}{L_3} + \frac{\Delta L_2 \Delta L_3}{L_2 L_3} + \frac{\Delta L_1 \Delta L_3}{L_1 L_3} + \frac{\Delta L_1 \Delta L_2}{L_1 L_2} + \frac{\Delta L_1 \Delta L_2 \Delta L_3}{L_1 L_2 L_3}. \quad \text{Eq (10)}$$

Substituting definition of longitudinal strain, Eq (3), into Eq (10),

$$S_V = S_{L_1} + S_{L_2} + S_{L_3} + S_{L_2} S_{L_3} + S_{L_1} S_{L_3} + S_{L_1} S_{L_2} + S_{L_1} S_{L_2} S_{L_3}, \quad \text{Eq (11)}$$

and assuming the body is isotropic (strain equal in all directions), then volumetric strain becomes:

$$S_V = 3S_L + 3S_L^{\,2} + S_L^{\,3}. \quad \text{Eq (12)}$$

If strain is small, then last two terms can be neglected and volumetric strain is approximately equal to three times the linear strain,

$$S_V \approx 3S_L. \quad \text{Eq (13)}$$

The error associated with Eq (13) is roughly equivalent to the linear strain. So that with a linear strain of 1%, the actual strain is about 1% more than that given by the above equation; with a linear strain of 10%, the actual strain is about 10% greater; and so on. However, there is no error associated with Eq (12) if the material is isotropic with respect to strain.

APPENDIX B – SI METRIC CONVERSION FACTORS

psi	X	6.894 757	E + 00	= kPa
in.	X	2.54*	E + 00	= cm
Btu	X	1.055 056	E + 00	= kJ
ft	X	3.048*	E – 01	= m
ft3	X	2.831 685	E – 02	= m3
lbm	X	4.535 924	E – 01	= kg
^{o}F	(^{o}F – 32)/1.8			= ^{o}C
ton	X	9.071 847	E – 01	= Mg

*Conversion factor is exact.

NOMENCLATURE

L = Length, cm
P = Pressure, psia
P_L = Langmuir pressure constant, psia
S = Strain, dimensionless
S_L = Longitudinal strain, dimensionless
S_{max} = Langmuir pressure strain constant; strain at infinite pressure, dimensionless
S_t = Langmuir time strain constant, strain at infinite time, dimensionless
S_v = Volumetric strain, dimensionless
t = Time, hours
t_L = Langmuir time constant, hours
V = Volume, cm^3
ΔL = Change in length, cm
ΔV = Change in volume, cm^3

ACKNOWLEDGMENTS

This work has been funded by Battelle Energy Alliance, the prime contractor at the Idaho National Laboratory. The authors wish to express their thanks to the management of the Idaho National Laboratory for funding this work and allowing its publication. We also express our gratitude to Mike Glasson of Andalex Resources and Greg Gannon of Kennecott for help in the collection of the coal samples.

REFERENCES CITED

1. Gray, I., 1987: "Reservoir Engineering in Coal Seams: Part 1 – The Physical Process of Gas Storage and Movement in Coal Seams," paper SPE 12514, *SPE Reservoir Engineering* (February 1987) 28-34.

2. Sawyer, W.K. and G.W. Paul, 1990: "Development and Application of a 3D Coalbed Simulator," paper CIM/SPE 90-119, presented at the 1990 International Technical Meeting hosted jointly by the Petroleum Society of CIM and the Society of Petroleum Engineers, Calgary, Alberta, Canada, 10-13 June.

3. Seidle, J.P. and L.G. Huitt, 1995: "Experimental Measurement of Coal Matrix Shrinkage Due to Gas Desorption and Implications for Cleat Permeability Increases," paper SPE 30010, presented at the 1995 International Meeting on Petroleum Engineering, Beijing, China, 14-17 November.

4. Palmer, I. and J. Mansoori, 1998: "How Permeability Depends on Stress and Pore Pressure in Coalbeds: A New Model," paper SPE 52607, *SPE Reservoir Evaluation & Engineering* (December 1998) 539-544.

5. Pekot, L.J. and S.R. Reeves, 2003: "Modeling the Effects of Matrix Shrinkage and Differential Swelling on Coalbed Methane Recovery and Carbon Sequestration, paper 0328 presented at the 2003 International Coalbed Methane Symposium, University of Alabama, Tuscaloosa, Alabama, May 2003.

6. Shi, J.Q. and S. Durucan, 2003: "Changes in Permeability of Coalbeds During Primary Recovery – Part 1: Model Formulation and Analysis," paper 0341 presented at the 2003 International Coalbed Methane Symposium, University of Alabama, Tuscaloosa, Alabama, May 2003.

7. Harpalani, S. and R.A. Schraufnagel, 1990: "Influence of Matrix Shrinkage and Compressibility on Gas Production From Coalbed Methane Reservoirs," paper SPE 20729, presented at the 1990 SPE Annual Technical Conference and Exhibition, New Orleans, Louisiana, 23-26 September.

8. Levine, J.R., 1996: "Model study of the influence of matrix shrinkage on absolute permeability of coal bed reservoirs," *Coalbed Methane and Coal Geology*, R Gayer and I. Harris (eds.) 1996, Geological Society Special Publication No. 109, 197-212.

9. Zutshi A. and S. Harpalani, 2004: "Matrix Swelling with CO_2 Injection in a CBM Reservoir and Its Impact on Permeability of Coal," paper 0425 presented at the 2004 International Coalbed Methane Symposium, University of Alabama, Tuscaloosa, Alabama, May 2004.

10. Chikatamarla, L. and M.R. Bustin, 2004: "Implications of Volumetric Swelling/Shrinkage of Coal in Sequestration of Acid Gases," paper 0435, proceedings of the 2004 International Coalbed Methane Symposium, paper 0360, University of Alabama, Tuscaloosa, Alabama, May 2004.

11. Robertson, E.P. and R.L. Christiansen, 2004: "Optically-based Strain Measurement of Coal Swelling and Shrinkage," paper 0417 presented at the 2004 International Coalbed Methane Symposium, University of Alabama, Tuscaloosa, Alabama, May 2004.

12. Stricker, G.D. and M.S. Ellis, 1999: "Coal Quality and Geochemistry, Powder River Basin, Wyoming and Montana," 1999 Resource Assessment Of Selected Tertiary Coal Beds And Zones In The Northern Rocky Mountains And Great Plains Region, Part I: Powder River Basin, *in* U.S. Geological Survey Professional Paper 1625-A.

13. *Annual Review and Forecast of Utah Coal, Production and Distribution – 2003*, prepared by the Utah Energy Office, Department of Natural Resources, printed October 2004.

14. Vorres, K.S., 1990: *Users Handbook for The Argonne Premium Coal Sample Program*, www.anl.gov/PCS/report/part1.html.

15. Pekot, L.J. and S.R. Reeves, 2002: "Modeling Coal Matrix Shrinkage and Differential Swelling with CO_2 Injection for Enhanced Coalbed Methane Recovery and Carbon Sequestration Applications," topical report, Contract No. DE-FC26-00NT40924, U.S. DOE, Washington, DC (November 2002).

16. Bustin, M., 2002: "Research Activities on CO_2, H_2S, and SO_2 Sequestration at UBC," Coal-Seq I Forum, Houston Texas, 14-15 March.

17. Reeves, S.R., 2003: "Enhanced CBM recovery, coalbed CO_2 sequestration assessed," *Oil & Gas Journal* (July 14) 49-53.

TABLES

Table 1. Coal strain values as reported by previous researchers.

Author	Gas	Strain		Pressure, psi
		Type	Value, percent	
Gray, 1987	CO_2	Longitudinal	1.0%	800
	CH_4	Longitudinal	0.06%	800
Harpalani and Schraufnagel, 1990	CH_4	Volumetric	0.6%	1000
Seidle and Huitt, 1995	CO_2	Volumetric	0.8%	800
Levine, 1996	CO_2	Longitudinal	0.5%	750
	CH_4	Longitudinal	0.2%	1000
Zutshi and Harpalani, 2004	CO_2	Volumetric	1.1%	750
	CH_4	Volumetric	0.5%	1000
Chikatamarla and Bustin, 2004	CO_2	Volumetric	2.41%	800
	CH_4	Volumetric	0.49%	1000

Table 2. Properties of coal samples collected and used in this research as ascertained from various analyses on an “as received” basis.

	Powder River basin, subbituminous		Eastern Utah, high-volatile bituminous		
	Anderson	Canyon	Gilson	Sunnyside	Aberdeen
Proximate Analysis wt%:					
Moisture	26.60	20.36	7.52	4.61	3.71
Ash	6.18	24.50	2.99	19.30	3.38
Volatile Matter	30.99	24.46	37.42	31.14	41.49
Fixed Carbon	36.23	30.68	52.07	44.95	51.42
Total	100.00	100.00	100.00	100.00	100.00
Ultimate Analysis wt%:					
Moisture	26.60	20.36	7.52	4.61	3.71
Hydrogen	2.08	1.83	3.86	3.68	4.56
Carbon	50.57	41.96	71.66	62.38	75.74
Nitrogen	0.43	0.34	1.36	0.80	1.60
Sulfur	0.27	0.54	0.49	1.37	0.59
Oxygen	13.87	10.47	12.12	7.86	10.42
Ash	6.18	24.50	2.99	19.30	3.38
Total	100.00	100.00	100.00	100.00	100.00
Heating Value, Btu/lb					
Measured	8,514	6,939	12,437	10,788	13,685
Literature values	8,220 [12]	—	12,000 [13]	—	12,300 [13]
Vitrinite Reflectance	0.24	0.28	0.53	0.62	0.54

Table 3. Langmuir strain constants for sorption-induced strain for Anderson and Gilson coals at 80° F.

Gas	Coal	Langmuir strain constants		R^2 value for curve fit
		S_{max}	P_L	
CO_2	Anderson	0.03447	529.19	0.9985
	Gilson	0.01596	581.32	0.9972
CH_4	Anderson	0.00777	618.98	0.9997
	Gilson	0.00891	1153.08	0.9981
N_2	Anderson	0.00429	1891.44	0.9989
	Gilson	0.00112	348.41	0.8914

FIGURES

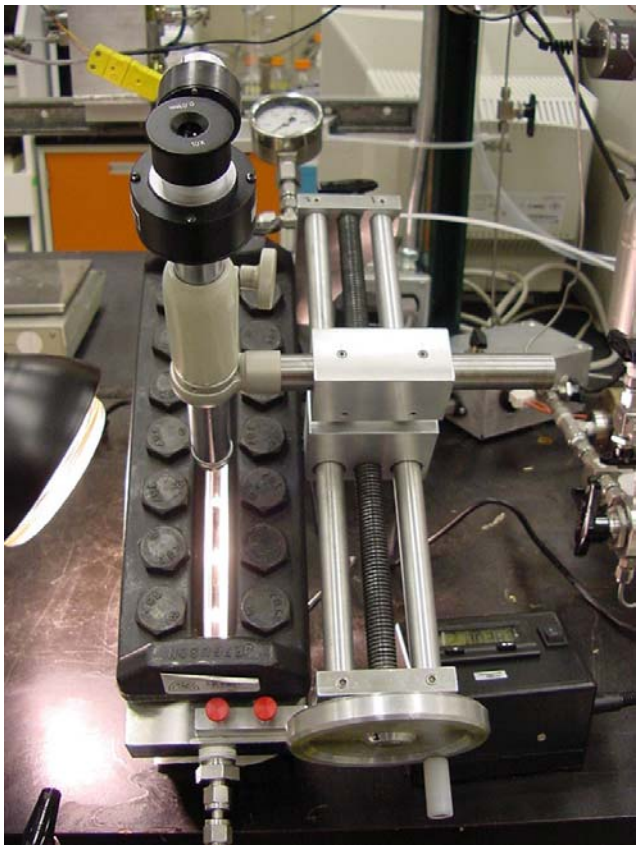

Figure 1. Photograph of the apparatus developed to measure the strain of multiple samples without the use of strain gauges.

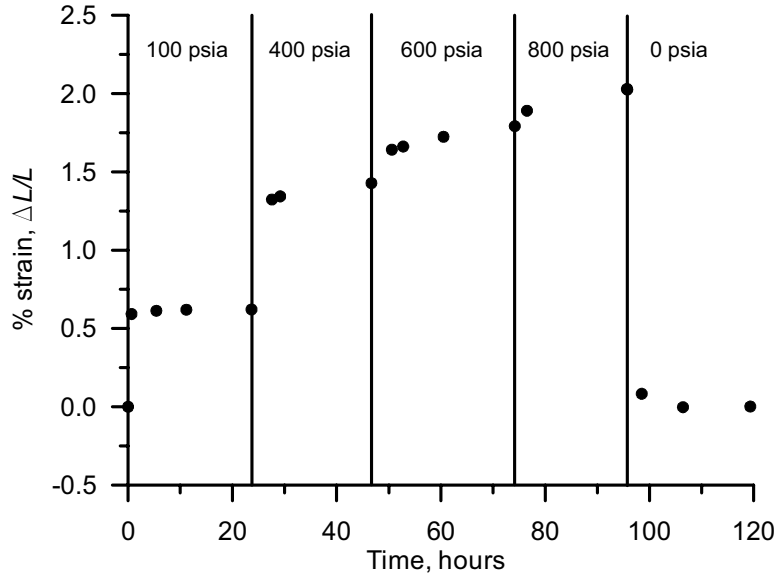

Figure 2. Graph of Anderson seam coal strain with respect to time under different carbon dioxide pressures.

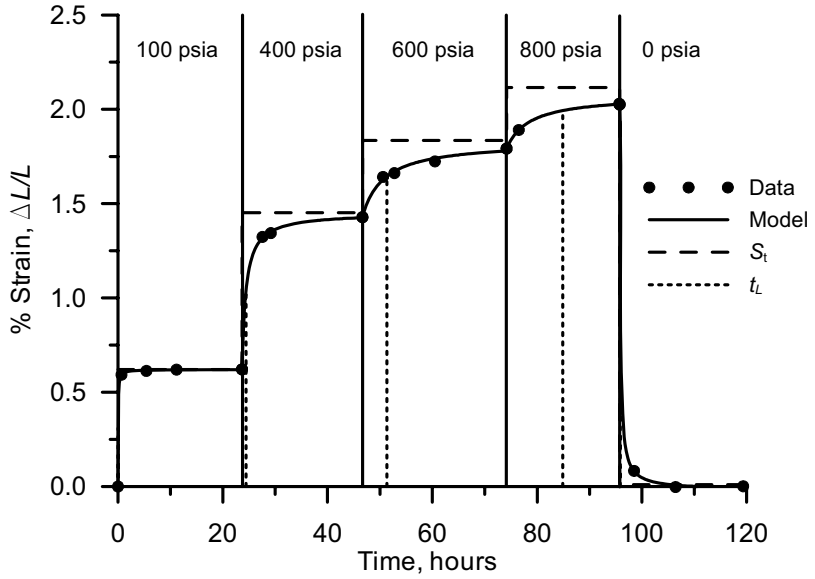

Figure 3. Graph of Anderson seam coal strain with respect to equilibration time under different carbon dioxide pressures. Also shown are the Langmuir-type model with corresponding constants.

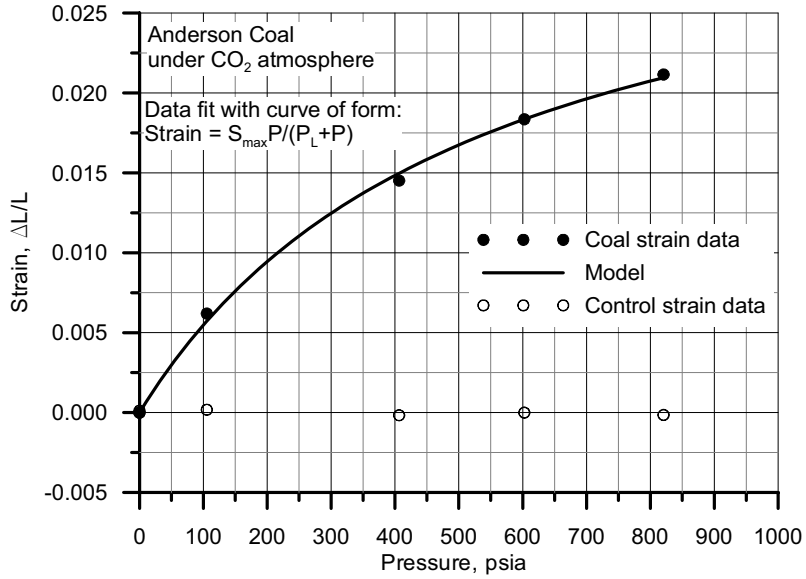

Figure 4. Measured Longitudinal strain using coal from the Anderson seam, Powder River basin of Wyoming under various CO_2 pressures. Also shown is the measured strain of a stainless steel sample used as a non-reactive control.

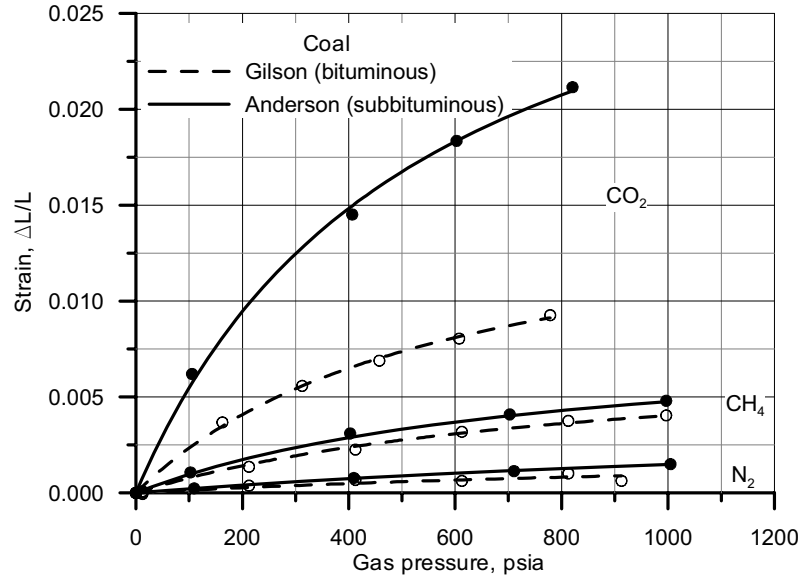

Figure 5. Strain curves for two different coals subjected to three different pure gases at various pressures.

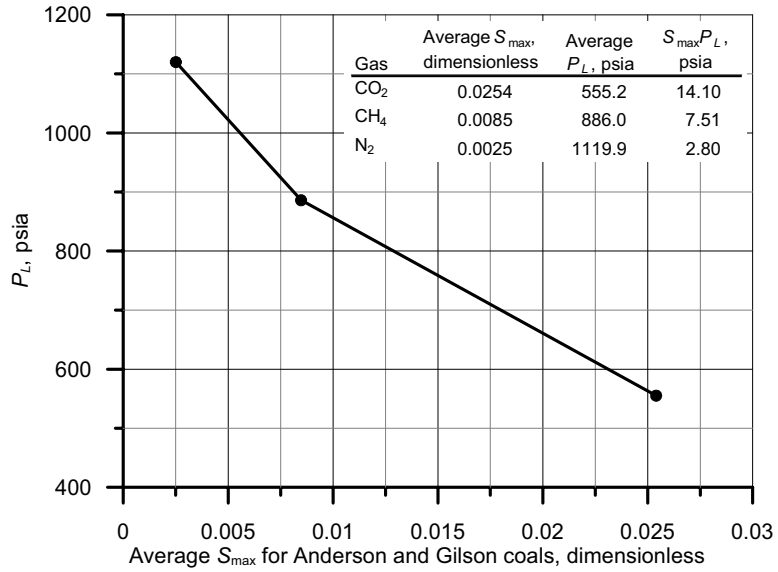

Figure 6. The relationship between the average Langmuir strain, P_L, and the average maximum strain for two different coals using three gases.

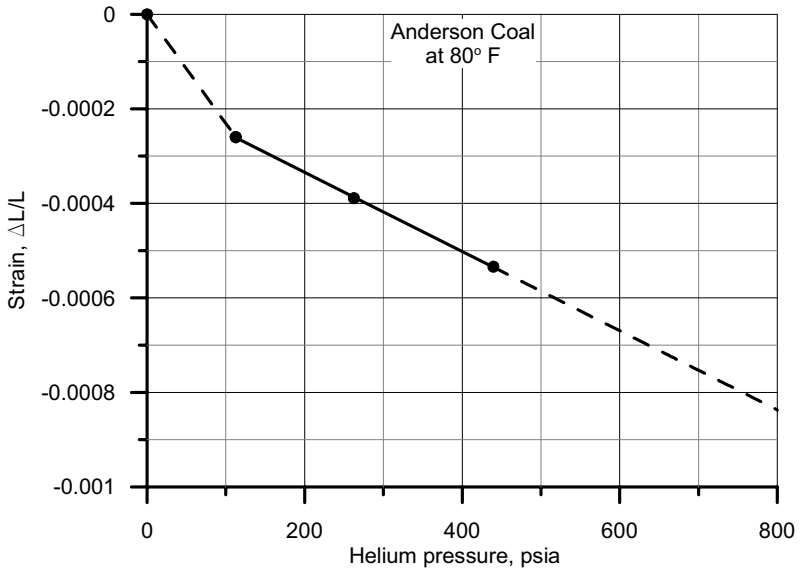

Figure 7. Longitudinal strain of Anderson (subbituminous) coal induced by various helium gas pressures at a constant temperature of 80 °F.

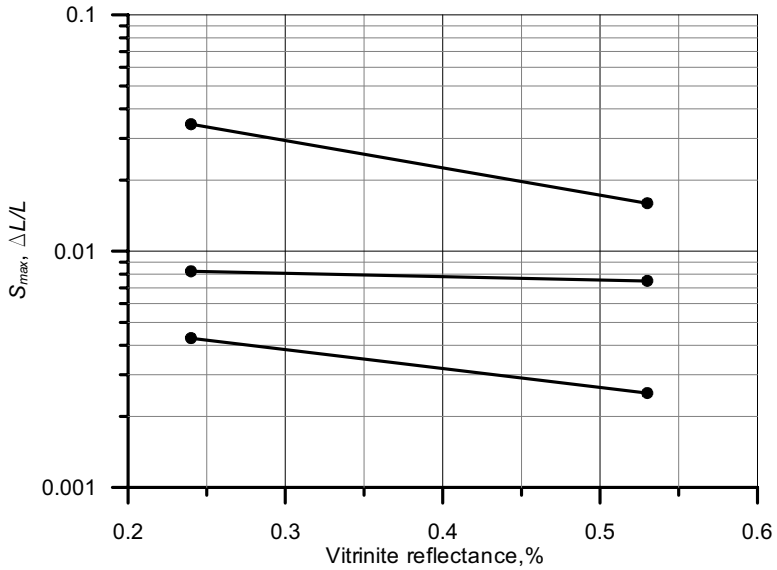

Figure 8. Graph of maximum strain and vitrinite reflectance showing trend toward lower strains as vitrinite reflectance (coal maturity) increases.

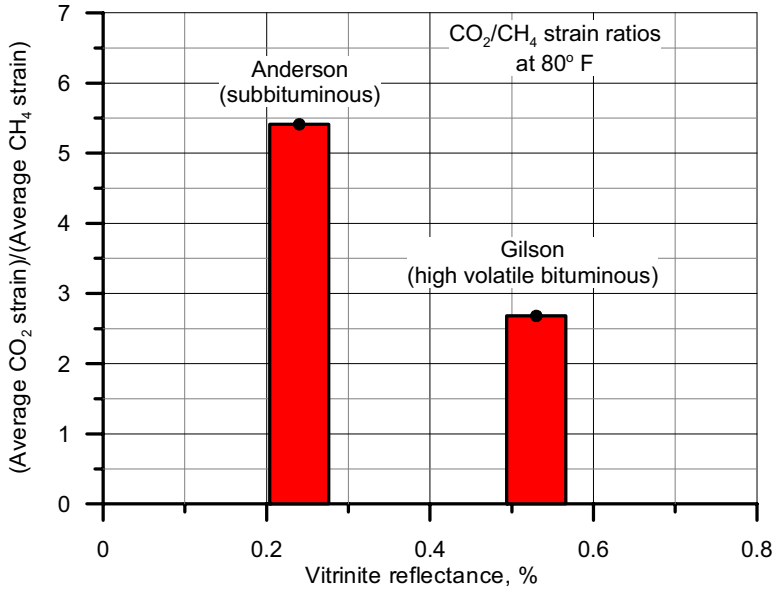

Figure 9. Average CO_2/CH_4 strain ratios for two coals of distinct ranks showing a decrease in the CO_2/CH_4 strain ratio with an increase in coal rank.